Phosphorylated nucleolar Tau protein is related to the neuronal in vitro differentiation

Article *in* Gene · April 2018

DOI: 10.1016/j.gene.2018.04.051

6 authors, including:

Concetta Federico
University of Catania
75 PUBLICATIONS **919** CITATIONS
SEE PROFILE

Laura Gil Alberdi
Universidad Alfonso X el Sabio
8 PUBLICATIONS **118** CITATIONS
SEE PROFILE

Francesca Bruno
University of Catania
6 PUBLICATIONS **22** CITATIONS
SEE PROFILE

Velia D'Agata
University of Catania
199 PUBLICATIONS **2,937** CITATIONS
SEE PROFILE

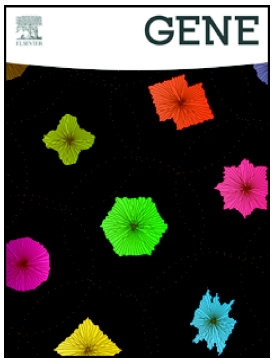

Phosphorylated nucleolar Tau protein is related to the neuronal in vitro differentiation

Concetta Federico, Laura Gil, Francesca Bruno, Agata Grazia D'Amico, Velia D'Agata, Salvatore Saccone

PII: S0378-1119(18)30425-6
DOI: doi:10.1016/j.gene.2018.04.051
Reference: GENE 42775

To appear in: *Gene*

Received date: 15 October 2017
Revised date: 6 April 2018
Accepted date: 18 April 2018

Please cite this article as: Concetta Federico, Laura Gil, Francesca Bruno, Agata Grazia D'Amico, Velia D'Agata, Salvatore Saccone , Phosphorylated nucleolar Tau protein is related to the neuronal in vitro differentiation. The address for the corresponding author was captured as affiliation for all authors. Please check if appropriate. Gene(2017), doi:10.1016/j.gene.2018.04.051

Phosphorylated nucleolar Tau protein is related to the neuronal *in vitro* differentiation

Concetta Federico[1#], Laura Gil[2#], Francesca Bruno[1], Agata Grazia D'Amico[3,4], Velia D'Agata[3], Salvatore Saccone[1*]

[1]*Department of Biological, Geological and Environmental Sciences, University of Catania, Italy.*

[2]*Department of Genetics, Medical School, University "Alfonso X el Sabio", Madrid, Spain.*

[3]*Department of Biomedical and Biotechnological Sciences, University of Catania, Italy.*

[4]*Department of Human Science and Promotion of Quality of Life, San Raffaele Open University of Rome, Italy*

# These authors contributed equally.

***** *Corresponding author*: **Salvatore Saccone, PhD**
Department of Biological, Geological and Environmental Sciences
Via Androne, 81
95124 Catania
Italy

Tel +39.095.7306037
e-mail saccosal@unict.it

RUNNING TITLE: Tau protein and nucleolar activity

ABSTRACT

Tau is a multifunctional protein, originally identified as a cytoplasmic protein associated with microtubules. It is codified by the *MAPT* gene, and the alternative splicing, in the neuronal cells, results in six different isoforms. Tau was subsequently observed in the cell nucleus, where its function is not yet clearly understood. Here, we studied the *MAPT* gene and the cellular localization of the AT8 and Tau-1 epitopes of Tau protein, in the SK-N-BE cell line, which differentiates in neuronal-like cells after retinoic acid treatment. These epitopes correspond to the phosphorylated Ser202/Thr205 and unphosphorylated Pro189/Gly207 amino acid residues, respectively, possibly involved in conformational changes of the protein. Our results demonstrated the presence of the smaller Tau isoform (352 amino acids), whose amount increases in differentiated SK-N-BE cells, with Tau-1/AT8 nuclear distribution related to the differentiation process. Tau-1 showed a spot-like nucleolar localization, in both replicative and differentiated cells, while AT8 was only detected in the differentiated cells, diffusely occupying the entire nucleolar region. Moreover, in the replicative cells exposed to actinomycin-D, AT8 and Tau-1 move to the nucleolar periphery and colocalize, in few spots, with the upstream binding transcription factor (UBTF). Our results, also obtained with lymphocytes exposed to the mitogenic compound phytohaemagglutinin, indicate the AT8 epitope of Tau as a marker of neuronal cell differentiation, whose presence in the nucleolus appears to be related to rDNA transcriptional inactivation.

ABBREVIATIONS LIST

Act-D	Actinomycin-D
ACTB	Actin-b
AD	Alzheimer's disease
AT8	Tau epitope with phosphorylated Ser202/Thr205 residues
CNS	Central nervous system
DAPI	4′,6-diamidino-2-phenylindole
DFC	Dense fibrillar component (of the nucleolus)
EDTA	Ethylene diamine tetraacetic acid
EGTA	Ethylene glycol tetraacetic acid
ETS	External transcribed spacer (in the rRNA gene cluster)
FBL	Fibrillarin
FC	Fibrillar centre (of the nucleolus)
FITC	Fluorescein isothiocyanate
GC	Granular component (of the nucleolus)
IF	Immunofluorescence

ITS1	Internal transcribed spacer-1 (in the rRNA gene cluster)
MAPT	Microtubule-associated protein Tau gene
MBD	Microtubule binding domain (of the Tau protein)
NFT	Neurofibrillary tangles
NOR	Nucleolar Organizing Regions
PBS	Phosphate buffered saline
PCR	Polymerase Chain Reaction
PHA	Phytohaemagglutinin
PNS	Peripheral nervous system
PRD	Proline-rich domain (of the Tau protein)
qRT-PCR	Quantitative Reverse Transcribed PCR
RA	Retinoic acid
rDNA	Ribosomal gene cluster
RPMI 1640	Roswell Park Memorial Institute medium
RQ	Relative quantification
Tau-1	Tau epitope with non-phosphorylated Pro189/Gly207 residues
TRITC	Tetramethylrhodamine
UBTF	Upstream binding transcription factor

KEYWORDS
Tau-1; AT8; *MAPT* gene; cell differentiation; rRNA genes; cell nucleus; neurons.

1. Introduction

Tau is a native unfolded protein with a flexible structure, discovered forty years ago as a protein associated with microtubules (**Weingarten et al., 1975**). It plays an important role not only in the cytoplasm, stabilizing microtubules and participating in axonal metabolism **(Goode et al., 1997; Dixit et al., 2008)**, but also in the cell nucleus (**Loomis et al, 1990**), where interaction with chromatin has been shown **(Sjöberg et al., 2006; Sultan et al., 2011; Hernàndez-Ortega et al., 2015; Mansuroglu et al., 2016).** It is encoded by the microtubule-associated protein Tau (*MAPT*) gene, which yields three transcripts of 2, 6 and 9 kb, with the 2 kb transcript observed in the cell nucleus (**Bukar Maina et al., 2016**).

In the central nervous system (CNS), Tau protein is largely present in six different isoforms, due to alternative splicing of exon 2 (E2), exon 3 (E3), and exon 10 (E10), with the largest composed of 441 amino acids. It is structurally subdivided into four parts: the N-terminal acidic region, the proline-rich domain (PRD), the microtubule binding domain (MBD) and the C-terminal region. The different uses of E2 and E3 determine the formation of a protein with 0, 1 or 2 repeats (called 0N, 1N and 2N) in the amino-terminal acidic region and the use of E10 determines the presence of three or four repeats (called 3R and 4R) in the MBD. The different combination of E2, E3, and E10 defines six Tau isoforms called 0N3R, 1N3R, 2N3R, 0N4R, 1N4R, and 2N4R (**Buée et al., 2000**; **Andreadis, 2005; Wang and Mandelkow, 2016; Bukar Maina et al., 2016**). The alternative splicing of the *MAPT* gene, in human brain and neuroblastoma cells **(Goedert et al., 1989; Loomis et al., 1990),** results in protein isoforms visible in a western blot as a series of closely spaced bands, with a size greater than about 50 kDa.

Conformational changes of Tau protein are determined by site-specific phosphorylations **(Avila, 2009),** allowing the acquisition of transitory structures **(Von Bergen et al., 2005; Jeganathan et al., 2008)** able to interact with multiple different proteins as well as with DNA and RNA **(Qi et al., 2015; Wang et al., 2006)**. Tau protein is phosphorylated by several serine/threonine kinase proteins, some of them related to abnormal Tau hyperphosphorylation, such as PKA, CaMKII, GSK-3β and cdk5. In particular among these proteins, GSK-3β plays an important role in both physiological and pathological phosphorylation (**Wang et al., 2007; Hanger and Noble, 2011**). In addition, deregulation of protein phosphatases, such as PP2A, is of extreme importance because their activity is often regulated by kinase-dependent phosphorylation (**Wang et al., 2007**).

Phosphorylations are involved in the formation of neurofibrillary tangles (NFT) that clinically define Alzheimer's disease (AD) and its various stages (**Braak and Braak, 1991**). However, only a few epitopes of Tau have been described in the nucleus, such as the phosphorylated AT8 (pSer202/Thr205) and AT100 (pThr212/Ser214) **(Rossi et al., 2008; Hernàndez-Ortega et al., 2015; Gil et al., 2017),** and the non-phosphorylated Tau-1 (Pro189/Gly207 residues), with the latter specifically immunolocalized in the nucleolus of neuronal and non-neuronal cells **(Loomis et al., 1990; Thurston et al., 1996; 1997; Sjoberg et al., 2006; Rossi et al., 2008).** Indeed, the non-

phosphorylated epitope Pro189/Gly207 of Tau was localized in the nucleolus of human fibroblast and HeLa cells, where it partially colocalized with alpha satellite DNA from pericentromeric chromatin, suggesting a role in the organization of the nucleolar heterochromatin (**Sjoberg et al., 2006**).

The nucleolus is the sub-nuclear region where rRNA synthesis and ribosomal assembly takes place. It is composed of three different regions, namely the fibrillar centre (FC) surrounded by the dense fibrillar component (DFC), and the granular component (GC) that, in turn, surrounds the FC/DFC region (**Boisvert et al., 2007; Bártová et al., 2010; Denissov et al., 2011; Smirnov et al., 2016**). The FC corresponds to the Nucleolar Organizing Regions (NORs), also detectable in the mitotic chromosomes and defining the chromatin with transcriptionally-active rDNA repeats (**McStay, 2016**), endowed with a non-nucleosomal euchromatic state in the interior of the nucleolus, as demonstrated by psoralen photocrosslinking (**Conconi et al., 1989**). In addition to these three functional subregions, the nucleolus is characterized by the presence of large heterochromatic blocks, generally located at the periphery of the GC, composed by the centromeric regions of the chromosomes involved in nucleolus formation, and by the heterochromatic stably silenced rRNA genes (**Lucchini and Sogo, 1992; Thiry and Lafontaine, 2005**; **Grummt, 2007; Sanij and Hannan, 2009; Mangan et al., 2017**). Indeed, the nucleolus contains rRNA genes, but a number of these genes are constitutively unexpressed, being silenced by epigenetic modifications involving methylation of the cytosine in the rDNA repeats (**Akhmanova et al., 2000**; **Sanij and Hannan, 2009**; **Parlato and Kreiner, 2013; D'Aquila et al., 2017**). Replicative cells are endowed by a high number of rRNA genes (about 50%) transcribed by RNA polymerase I, contrary to the differentiated cells, endowed by a low number (about 10%) of active rRNA genes (**Sanij and Hannan, 2009**; **Takada and Kurisaki, 2015**). Indeed, it was recently demonstrated that a downregulation of rDNA transcription is one of the mechanisms strictly related to the cell differentiation program (**Hayashi et al., 2014**).

In the present work, we studied nuclear Tau in the human neuroblastoma cell line SK-N-BE, which is able to differentiate in neuronal-like cells when induced by retinoic acid (**Leotta et al., 2014**). We analyzed the non-phosphorylated Pro189/Gly207 and the phosphorylated pSer202/Thr205 epitopes, detected with the antibodies Tau-1 and AT8, respectively. Moreover, we identified and quantified the Tau isoforms expressed in the replicative and differentiated SK-N-BE cells. The relevance of the obtained results, with respect to the nucleolar activity and cell differentiation, is discussed.

2. Materials and methods

2.1. Cell cultures

The human neuroblastoma cell line SK-N-BE (**Biedler et al., 1978**) and human peripheral blood lymphocytes were cultured in RPMI 1640 medium, supplemented with 10% fetal bovine serum (FBS) (20% for lymphocytes), 1% antibiotic Penicillin/Streptomycin (100 U/ml; 100 □g/ml) and 1% L-Glutamine, at 37°C, with 5% CO_2. To obtain replicative lymphocytes, the culture was performed with medium containing 3% phytohaemagglutinin (PHA) (GIBCO cat. n. 10576-015) for 72 hours. Human lymphocytes were obtained, from healthy volunteers, by venous blood sampling and then put into heparinised tubes. All procedures performed in the present study involving human participants were in accordance with the ethical standards of the institutional and/or national research committee and with the 1964 Helsinki declaration and its later amendments or comparable ethical standards. Signed informed consent forms were obtained from all the volunteer subjects.

SK-N-BE cells were differentiated in neuronal-like cells with a treatment of 10 µM retinoic acid (RA) (Sigma–Aldrich Cat. n. R2625) added to the culture medium every 72 hours (day 0, 3, 6, 9) to obtain differentiated cells on the 12^{th} day of treatment (**D'Alessio et al., 1995; Andres et al., 2013; Leotta et al., 2014**). Replicative SK-N-BE cells were incubated for 1 hour with 0.05 µg/ml of actinomycin-D (Act-D), before harvesting, to obtain the block of transcription (**Perry and Kelley, 1970; Bensaude, 2011**).

2.2. Cell preparation and immunofluorescence analysis

Immunofluorescence (IF) experiments were performed as previously described (**Maugeri et al., 2016**). Briefly, SK-N-BE cells were cultured on glass chamber-slides and fixed with 4% paraformaldehyde for 20 min at room temperature. Human lymphocytes were cytocentrifuged on glass slides and then fixed as above.

Cells were washed with phosphate buffered saline (PBS) and incubated for 15 min in PBS containing 0.5% Triton X-100. Immunodetections were performed by incubation with the specific antibody at the dilution suggested by the manufacturers. Before the incubation with primary antibody, a preincubation step of 1 hour at 37°C with blocking solution (non-fat dry milk or bovine serum albumin 1%) was carried out. The antibodies used were Tau-1 (Millipore Cat. MAB3420), to detect Pro189/Gly207 residues, and AT8 (Thermo Scientific Cat. MN1020) to detect pSer202/Thr205. Moreover, antibodies against UBTF (NBP1-82545), GAP-43 (Millipore Cat. AB5312) and fibrillarin LS-C204517 (Clone 38F3) were used to evaluate the different status of the SK-N-BE cells. Dual colour IF was also performed by using mouse anti-Tau-1 or AT8 antibodies together with the rabbit anti-UBTF antibody.

After overnight incubation and additional PBS washes, cells were incubated at 37°C for 1 hour with FITC-conjugated sheep anti-mouse secondary antibody (Sigma-Aldrich, 1:100 dilution in blocking solution) together, in the case of the dual colour IF, with the TRITC-conjugated goat anti-rabbit (Sigma-Aldrich, 1:400 dilution in blocking solution).

Experiments were repeated at least three times. The results were analysed with confocal laser scanning microscopy (CLSM) (Zeiss LSM700) and images were captured at 400x and 630x magnification, and ZEN-2010 software was used for image acquisition and analysis.

2.3. Reverse Transcription PCR

To identify the different isoforms of *MAPT* gene present in the SK-N-BE cells, RNA was extracted using TRI Reagent (Sigma-Aldrich, St. Louis, USA). cDNAs, obtained by retrotranscription (SuperScript III First-Strand Synthesis SuperMix, Invitrogen), were amplified by PCR (Taq DNA Polymerase, recombinant, Invitrogen) with the following conditions: 94 °C for 5 min, followed by 35 cycles at 95 °C for 30 sec, 60 °C for 30 sec, and 72 °C for 40 sec. In the case of longer expected amplified segments, the elongation step was increased (72 °C for 2 min 30 sec). The primers used to identify the exons are shown in **Table 1**.

The amplified DNA segments were electrophoresed on agarose gel (from 0.8 to 2%, depending on the expected fragment sizes) with SYBR Safe DNA Gel Stain, and visualized with a Safe imager blue-light transilluminator (Thermo Fisher Scientific, USA).

2.4. Quantitative RT-PCR

RNAs and cDNA were obtained, as described above, from replicative and differentiated cells. Detection and quantification of *MAPT* transcripts were carried out by qPCR (with the StepOne instrument from Applied Biosystems, USA) using specific primers (**Table 1**). Experiments were performed with Power SYBR Green PCR Master Mix (Applied Biosystems, Life Technologies, UK) according to the manufacturer's instructions, with the specific annealing temperature. Experiments were repeated at least three times.

To assess the different levels of *MAPT* transcripts, we employed the relative quantification method with actin-b (ACTB, from Sigma-Aldrich) as an endogenous control, and replicative SK-N-BE cells as a calibrator reference. Data were analysed using the Ct value obtained for each sample. This was normalized with the Ct value of the endogenous control (ACTB) obtaining the ΔCt. Normalizing the ΔCt of the sample of interest with that of the calibrator, we obtained the ΔΔCt. Finally, to determine the relative quantification (RQ) of each sample, we used the $2^{-\Delta\Delta Ct}$ formula.

Expression levels of *rRNA* genes in differentiated *vs* replicative SK-N-BE cells, and *fibrillarin* gene in PHA induced/not induced lymphocytes were obtained by qRT-PCR using the "SuperScript III Platinum Sybr green One-step qRT-PCR" kit (Invitrogen) and the StepOne instrument (Applied Biosystems, USA). To evaluate the rRNA transcriptional level we used primers (**Table 1**) to amplify a segment from the external transcribed spacer (ETS) of the rRNA gene cluster. Moreover, we used other primers (see **Table 1**) to amplify segments from the non-transcribed promoter region (negative control), and from the 18S rRNA, also present in the mature ribosomes (positive control). To quantify fibrillarin transcript we used primers (**Table 1**) previously described (**Koh et al., 2011**). ACTB

(Sigma-Aldrich) was used as an endogenous control and replicative SK-N-BE cells, and not induced lymphocytes as a reference samples. Then, the RQ ratio was used to compare obtained data in the different cell treatments (**Federico et al., 2017a**).

2.5. Western Blot Analysis

Western blot analysis was performed according to the procedures previously described (**Maugeri et al., 2015**). Briefly, proteins were extracted with buffer containing 20 mM Tris (pH 7.4), 2 mM EDTA, 0.5 mM EGTA; 50 mM mercaptoethanol, 0.32 mM sucrose and a protease inhibitor cocktail (Roche Diagnostics) and phosphatase inhibitor cocktail (PhosSTOP Phosphatase Inhibitor, Roche) using a Teflon-glass homogenizer. The samples were then sonicated twice for 20 sec using an ultrasonic probe, followed by centrifugation at 10,000 g for 10 min at 4 °C. Protein concentrations were determined by the Quant-iT Protein Assay Kit (Invitrogen). Sample proteins (30 μg) were diluted in 2X Laemmli buffer (Invitrogen, Carlsbad, CA, USA), heated at 70°C for 10 min and then separated on a Biorad Criterion XT 4-15% Bis-tris gel (BIO-RAD) by electrophoresis and transferred to a nitrocellulose membrane (BIO-RAD). Blots were blocked using the Odyssey Blocking Buffer (LI-COR Biosciences) and probed with appropriate antibodies: mouse anti-AT8 (MN1020; 30 μg/ml), mouse anti-Tau-1 (MAB3420; 1:200), mouse anti-Tau-5 (sc-58860, Santa Cruz Biotechnology; 1:200) to detect total Tau (Ittner et al., 2009), and rabbit anti-β-tubulin (sc-9104, Santa Cruz Biotechnology; 1:500).

The secondary antibody goat anti-rabbit IRDye 800CW (#926-32211; LI-COR Biosciences) and goat anti-mouse IRDye 680CW, (#926-68020D; LI-COR Biosciences) were used at 1:20000. Blots were scanned with an Odyssey Infrared Imaging System (Odyssey). Densitometric analyses of blots were performed at non-saturating exposures and analysed using the ImageJ software (NIH, Bethesda, MD; available at http://rsb.info.nih.gov/ij/index.html). Values were normalized to β-tubulin, which was used as a loading control. No signal was detected when the primary antibody was omitted (data not shown).

For statistical analysis, data are represented as mean ± standard error (S.E.M). One-way analysis of variance (ANOVA) was used to compare differences among groups, and statistical significance was assessed by the Tukey–Kramer post hoc test.

3. RESULTS

To study the nuclear Tau in neuronal cell differentiation, we used the neuroblastoma SK-N-BE cell line, which differentiates in neuronal-like cells after retinoic acid treatment. We assessed cell differentiation with several methods, namely by visualization of very long cell protrusions resembling neuritic/dendritic extensions, variation in the morphology of NORs, and the presence/absence of specific proteins such as GAP-43 (located in the axonal extensions of the differentiated cells) and fibrillarin (located in the nucleolus of the replicative cells) (**Fig. 1**). We also verified the reduced level of rDNA expression in the differentiated SK-N-BE cells, analysing the RNA level of the external transcribed spacer (ETS) by means of qRT-PCR (**Fig. 2**). Our results showed in the differentiated cells a level of rDNA transcription of about 30% with respect to the replicative cells, confirming previous findings on a reduced rate of transcriptional activity during cell differentiation (**Sanij and Hannan, 2009**; **Takada and Kurisaki, 2015**).

3.1. Tau protein in the nucleolus of the SK-N-BE cells

Antibodies Tau-1 and AT8, detecting the same region of Tau protein without or with phosphorylation in the Pro189/Gly207 and the Ser202/Thr205 residues, respectively, were used to localize, by means of IF, these epitopes in the replicative and differentiated SK-N-BE cells. In the replicative cells, Tau-1 showed a number of small spots located in the nucleolar space, away from the nucleolar peripheral heterochromatin (**Fig. 3A**). More precisely, the large number (about 90%) of analysed nuclei showed from 8 to 12 fluorescent signals (8%, 24%, 39%, 15% and 4% of nuclei with 8, 9, 10, 11 or 12 signals, respectively), and the remaining (about 10%) less than 8 IF signals. In contrast, AT8 epitope was not detected in the nuclear or nucleolar region (**Fig. 3B**). In the differentiated cells, Tau-1 showed specific signals in the nucleolus but, in contrast to the pattern observed in the replicative cells, we detected few large spots in the inner part of the nucleolar space, away from the nucleolar periphery (**Fig. 3C**). The large number (about 95%) of analysed nuclei showed from 2 to 6 fluorescent signals (6%, 14%, 30%, 36% and 9% of nuclei with 2, 3, 4, 5 or 6 signals, respectively). The remaining nuclei (about 5%) showed only one or no IF signals. In the case of AT8, in all the differentiated cells, we observed specific signals, uniformly present throughout the nucleolar region (**Fig. 3D**). The nucleolar location of Tau-1 and AT8 was confirmed by dual-colour IF with UBTF (**Fig. 4a,e** and **4f** respectively).

Thus, Tau protein is present in the nucleolus of replicative and differentiated SK-N-BE cells, but with a different pattern depending on the phosphorylation status of the Ser202/Thr205 residues. Indeed, a dramatic change in the signal distribution during differentiation was detected, with AT8 only appearing in the differentiated neuronal-like cells.

3.2. Tau protein in the transcriptionally inhibited cells

Tau-1 and AT8 were analysed in the replicative SK-N-BE cells treated with actinomycin-D (Act-D), which determines, under the conditions used, the transcriptional inhibition of the RNApol-I (**Perry**

and Kelley, 1970; Bensaude, 2011). Tau-1 showed few spots at the nucleolar periphery indicating that Act-D determines the collecting and relocalization of the Tau protein containing the unphosphorylated Pro189/Gly207 residues (**Fig. 4C,c,c'**). The large number (about 88%) of the analysed nuclei showed from 4 to 6 fluorescent signals (27%, 46% and 15% of nuclei with 4, 5 and 6 spot signals, respectively). The remaining nuclei showed less than 4 (9%) or more than 6 (3%) IF signals. This protein distribution is similar but not identical to that observed in the differentiated cells; indeed, in this latter case signals are inside the nucleolus, while after Act-D exposure the signals are at the nucleolar periphery (compare **Fig. 4c'** ***vs*** **4e'**). The same type of relocalization was observed for UBTF, and dual-colour IF demonstrated colocalization of Tau-1 and UBTF at the nucleolar periphery following Act-D exposure of the SK-N-BE (**Fig. 4c**).

AT8, in the Act-D exposed cells, similarly to Tau-1, was detected as large spots at the nucleolar periphery, largely colocalizing with UBTF (**Fig. 4d**). The large number (about 85%) of analysed nuclei showed from 3 to 5 fluorescent signals (12%, 31% and 42% of the nuclei with 3, 4 or 5 signals, respectively). The remaining nuclei showed less than 3 (9%) or more than 5 (6%) IF signals. In addition a diffuse signal occupying part of the nucleolar region around the large spots was observed (**Fig. 4D,d,d'**). Thus, the nucleolar distribution of AT8, in the Act-D exposed cells, is very different with respect to the absence of signals of the replicative cells as well as with respect to the diffuse signal observed in the differentiated cells.

3.3. Tau protein in the mitotic cells

Tau-1 was observed in the metaphase chromosomes in replicative (**Fig. 4G**) and Act-D exposed cells (**Fig. 4K**), colocalizing with UBTF (**Fig. 4P**). During the anaphase, signals were also present in the two separated chromosomal groups (**Fig. 4I**). A large amount of AT8 was detected in the replicative cells, around the metaphasic and anaphasic chromosomes (**Fig. 4J**), with a signal distribution occupying the entire cell. In this latter case, no colocalization with UBTF was observed (**Fig. 4T**). It should be stressed that at the end of mitosis, AT8 completely disappeared from the cell, with its absence being evident in the interphase nuclei (**Fig. 4H,J**). Instead, the Act-D exposure of the replicative cells led to a large decrease in the AT8 epitope around the mitotic chromosomes, with only a very faint signal visible, and a concomitant increased level in the nucleolus (**Fig. 4L**).

3.4. Tau protein in human lymphocytes

Tau-1 and AT8 antibodies were used to detect Tau protein in human lymphocytes before (non-dividing cells, with very low transcriptional activity) and after (dividing cells with high transcriptional activity) PHA treatment. The transcriptional feature was assessed by the absence/presence of fibrillarin in the non-induced or PHA-induced lymphocytes, respectively (**Fig. 5C,F**), and by the transcriptional level of the *fibrillarin* gene (**Fig. 5G**). According to previous data (**Torelli et al., 1968; Dauphinais, 1981**), rDNA genes showed an increased transcriptional level in PHA-induced respect to

the non-induced lymphocytes (**data not shown**). Thus, we can compare our data with replicative/differentiated SK-N-BE cells with respect to PHA-induced/non-induced lymphocytes, taking into consideration the transcriptional activity and the cell cycle progression.

In the lymphocytes without PHA stimulation, Tau-1 signal was detected in a single large spot in correspondence to the small nucleolus present in these cells (**Fig. 5A**). A similar result was also observed with AT8, even if in this case few signals were also detected in the cytoplasm (**Fig. 5B**). In the PHA-induced lymphocytes, Tau-1 antibody detected a number of spots inside the nucleolus, which in these cells is very large (**Fig. 5D**) and transcriptionally active (**Fig. 5F,G**). The large number (about 95%) of analysed nuclei showed from 7 to 14 fluorescent signals (12%, 30%, 26% and 12% of the nuclei with 9, 10, 11 or 12 signals, respectively), and the remaining (about 5%) less than 7 IF signals. In the case of AT8, signals completely disappeared from the nucleolus, with only few signals present in the cytoplasm (not detected in all the cells, but only in about 20% of them) (**Fig. 5E**). Localization of tau protein (Tau-1, and AT8) in the nucleolus was confirmed by IF co-localization with UBTF (**Fig. 5**).

3.5. Identification of Tau isoforms in the SK-N-BE cells

To identify the isoforms of Tau present in the SK-N-BE cells, we performed RT-PCR with a number of different pairs of primers (**Table 1**) to define the exons retained in the mRNA of the *MAPT* gene (**Fig. 6A**).

The pairs of primers F1-R4 and F2-R4 were used to define the presence/absence of exons 2 and 3 (**Fig. 6A**), highlighting the N-terminal repeats of Tau protein called 0N, 1N and 2N (see Introduction). The size of the amplified segments indicated that the 0N repeat (DNA segment of 196 bp with F1-R4 primers) is largely present and that the 2N is not detectable (DNA segments of 370 bp and 202 bp with F1-R4 and F2-R4 primers, respectively, not present). In the case of the 1N repeat, the corresponding amplified DNA segment is only faintly visible (283 bp and 115 bp band size obtained with the primers F1-R4 and F2-R4, respectively) (**Fig. 6B**). These data were also confirmed by the quantitative RT-PCR (see below). Data obtained with the pairs of primers F4-R5, F4-R7 and F4-R9 showed that exon 4A and exon 6, as expected, are not present in the mRNA, even if a very faint DNA band is visible with the primers F4-R7 at a size (402 bp) compatible to the presence of exon 6 in the amplified segment (**Fig. 6B**). The primers F9/10-R12 (specific for exon 10 retention in the mRNA) and F9/11-R13 (specific for exon 10 exclusion in the mRNA) demonstrated that exon 10 is present or absent in the mRNA, thus highlighting the presence of at least two different isoforms of Tau containing the 3R or 4R repeats in the MBD region.

Results obtained with the pairs of primers F1-R11 and F1-R13 showed the presence of two bands, with a size corresponding to the mRNA coding for the isoforms with the smaller size (**Fig. 6C**). The mRNAs coding for the larger isoforms 2N3R, 1N4R and 2N4R are not present in the SK-N-BE cells, as demonstrated by the absence of the amplified segments larger than 850 bp and 1200 bp with

primers F1-R11 and F1-R13, respectively (**Fig. 6C**). Thus, the visible bands, also considering the quantitative RT-PCR results (see below), correspond to the 0N3R (689 bp or 1063 bp obtained with F1-R11 or F1-R13 primers, respectively) and to 0N4R (782 bp or 1156 bp obtained with F1-R11 or F1-R13 primers, respectively) isoforms. The presence of the 1N3R isoform (with an expected size very close to that of the 0N4R isoform) could be excluded given the data from qRT-PCR (see below).

In summary, our data highlight the presence of two smaller-sized Tau proteins endowed with the absence of the repeats at the N-terminal end, and with 3 or 4 repeats in the MBD region, corresponding to the 0N3R and 0N4R isoforms of Tau. Moreover, data obtained in replicative and differentiated SK-N-BE cells demonstrate the presence of the same isoforms in both types of cells. In the case of exon 6, faintly visible in some amplifications, we can assume the presence in these cells of a small amount of truncated forms of Tau, described in the literature, but again not very well studied.

3.6. Quantitative expression of MAPT gene and Tau protein

The relative quantification of both mRNA and protein of Tau was performed in the replicative *vs* differentiated SK-N-BE cells (**Fig. 7** and **Fig. 8**). Quantitative RT-PCRs were performed using primers specific for the exons corresponding to 0N, 1N, 2N, 3R and 4R repeats (**Table 1**). The results demonstrated the presence of the 0N (**Fig. 7A**) and 3R (**Fig. 7B**) repeats at higher levels with respect to the others. Moreover, in the differentiated cells, there was an increased level of 0N3R mRNA of about 10 times higher than that present in the replicative cells (**Fig. 7C**), as well as for the total Tau protein, which increases about 8 times (**Fig. 8A**). The qRT-PCR demonstrated the absence or the very low levels of exons corresponding to the 1N and 2N repeats.

Tau-1 and AT8 epitopes were detected by western blot with cell homogenates from replicative, differentiated, and replicative after 1 hour of Act-D treatment SK-N-BE cells. Results demonstrated the presence of Tau protein with a size corresponding to the smallest isoform 0N3R (**Fig. 8**), according to the above qRT-PCR data. AT8 epitope, in all cases, was detected in larger amounts with respect to Tau-1, with AT8 being about 9 and 11 times higher than Tau-1 in the replicative and differentiated cells, respectively. In the case of Act-D exposed cells, this difference was even higher, with the amount of AT8 being about 25 times higher with respect to the Tau-1 (**Fig. 8B,C**).

In differentiated and Act-D induced cells, we detected an increasing level of Tau-1 and AT8 with respect to the replicative cells. More specifically, the amounts of Tau-1 and AT8 increased 2 and 2.5 times, respectively, in differentiated with respect to replicative cells (**Fig. 8B,C**). In the Act-D induced cells, with respect to the replicative ones, the increasing level of AT8 (about 3.5 times higher) was statistically highly significant (**Fig. 8C**), while the increasing level of Tau-1 was statistically not significant (**Fig. 8B**). It should be stressed that total Tau does not increase significantly after Act-D treatment, in contrast to the increased amount observed in differentiated cells (**Fig. 8A**).

4. DISCUSSION

Since its discovery, Tau protein has been repeatedly detected in the nucleus of neuronal as well as non-neuronal cells, even if its role in the nucleus is not yet well understood. Here, we showed the presence in the nucleolus of the smaller isoform of Tau and its correlation, depending on the phosphorylated status of the Ser202/Thr205 residues, with the *in vitro* neuronal-like differentiation of the SK-N-BE cells, indicating a possible role in nucleolar organization and rDNA transcriptional activity.

4.1. MAPT gene expression

We demonstrated that the largest amount of Tau in both replicative and differentiated SK-N-BE cells is the isoform 0N3R, with an increasing level in the differentiated cells. This isoform was also previously shown in other neuroblastoma cell lines (SH-SY5Y and SK-N-SH) (**Smith et al., 1995**) and is also known as the foetal Tau isoform, being the only one observed in the foetal brain (**Buée et al., 2000; Bukar Maina et al., 2016**). The presence of the 0N3R isoform in the replicative or differentiated SK-N-BE cells could be explained considering that the features of these cells are similar to that of the neuroblasts or of the early-differentiated neuronal cells present in the foetus. Thus, we can assume that in the SK-N-BE differentiation the switch to the longer Tau isoforms does not occur, possibly due to the limited vital time of these cells, and this differs from normal neuronal differentiation, which is longer, as previously proposed (**Smith et al., 1995**).

4.2. Unphosphorylated Tau-1 epitope, nucleolus and rRNA genes

Cell differentiation is related to chromatin reorganization in the nucleus in a process that allows the positioning of tissue-specific genes in the more appropriate nuclear compartment. It is well known that the peripheral and the inner part of the nucleus are largely occupied by the transcriptionally inactive or active genomic DNA, respectively (**Saccone et al., 2002; Federico et al., 2008; 2017b; Bernardi, 2015**), and the nucleolus seems to be involved in the nuclear chromatin organization (**Carmo-Fonseca et al., 2000**). The nucleolus is a dynamic structure that undergoes significant changes in its morphology depending on the cell cycle needs. In the replicative cells, the nucleolus shows a higher transcriptional activity, with about 50% of rRNA genes actively transcribed, and appears as multiple small nucleoli formed surrounding the active FC/DFC. These small nucleoli tend to fuse in only one nucleolus in slowly proliferating or differentiated cells **(Anastassova-Kristeva, 1977)**, with only a small number of rRNA genes, about 10%, are expressed with a large number of these genes present in a heterochromatic or methylated inactive form (**Sanij and Hannan, 2009; Takada and Kurisaki, 2015**). Along this line of evidence, Tau protein seems to play a role, possibly in the organization of the rRNA genes.

Our results showed that, in replicative cells, nuclear Tau with unphosphorylated Pro189/Gly207 residues (Tau-1 epitope) is arranged in a number of spots in the inner part of the nucleolus. It is also

present in the chromosomes at the metaphase and anaphase stage, largely colocalizing with the upstream binding transcription factor (UBTF). This highlights a direct or indirect interaction of Tau-1 with rDNA during the entire cell cycle. This is further confirmed by the concerted Tau-1 and UBTF reorganization in the nucleolus following Act-D exposure, as previously shown, in the case of UBTF, in other cell types (**Sobol et al., 2013; Mangan et al., 2017**). In the differentiated cells, Tau-1 was observed in a lesser number of dots, also in this case largely colocalizing with UBTF. Considering the central role of UBTF in rDNA transcription (**Qu et al., 2004**), we can speculate that Tau-1 may be involved in the organization and/or expression of the active rRNA genes.

Considering the positional correlation with NORs and UBTF and the previously reported properties of Tau to bind DNA (**Hua and He, 2003; Sjöberg et al., 2006; Wei et al., 2008; Violet et al., 2014; Mansuroglu et al., 2016; Qi et al., 2015; Wang et al., 2006**), we can hypothesize a role for Tau in helping UBTF in the binding of rDNA. Nonetheless, further work will be necessary to better understand the exact role of Tau-1 related to rRNA genes and the identification of the possible direct interaction with UBTF and/or rDNA.

4.3. Phosphorylated AT8 epitope and rRNA inactivation

The AT8 epitope (pSer202/Thr205 residues) is absent from the nucleolus of replicative cells, but is largely present during mitosis, around the metaphase/anaphase chromosomes. AT8 appears in the nucleolus when the transcriptional activity is blocked (Act-D exposed cells) or largely reduced (differentiated cells), thus highlighting a possible correlation with rDNA silencing. This role has also been confirmed by the colocalization of AT8 with UBTF (and indirectly with Tau-1) at the nucleolar periphery in the Act-D exposed cells.

Considering that AT8 is located around the mitotic chromosomes (in the replicative cells) and in the nucleolus of cells with low or no transcriptional activity (differentiated or Act-D induced cells), we speculate that AT8 antibody, in the neuroblastoma cells, detects two different types of the smallest Tau isoform 0N3R, characterized by different phosphorylation patterns, with a phosphorylation in the Ser202/Thr205 residues, and the others in different, undetected sites: one type is involved in the mitosis and the other in a process possibly related to the inactivation of the rRNA genes.

4.4. Tau-1 and AT8 in the nucleolus of lymphocytes

The nucleolar fusion occurring during cell differentiation requires the reorganization of most of the human chromosomes carrying rDNA, and specifically of the heterochromatic sequences on their p-arm, both proximal and distal to the rDNA. In differentiated cells, it has been suggested that the rDNA-associated heterochromatin plays a role in the maintenance of nucleolar structure (**Carmo-Fonseca et al., 2000).** Recently, a role for Tau in the structure and stability of the pericentromeric heterochromatin has been suggested **(Mansuroglu et al., 2016)**, and the present results with AT8 added further evidences to its role in the nucleolus.

When lymphocytes are in a non-replicative state, they show a small nucleolus, low transcriptional activity, and the presence of the Tau-1 and AT8 epitopes resembling the situation described in the differentiated SK-N-BE cells. Moreover, after the cell cycle activation by PHA induction, and the increase in transcriptional activity, the nucleolus increases in number and size, with Tau-1 evolving in the same pattern of signals observed in the replicative SK-N-BE cells. The nucleolar AT8, as in the case of the replicative SK-N-BE cells, disappears from PHA stimulated lymphocytes, possibly due to the activation of a higher number of rRNA genes. Thus, lymphocytes and SK-N-BE cells endowed with similar transcriptional activity (and rRNA gene expression) show the same pattern of Tau-1 and AT8 localization, indicating a possible general role of Tau protein related to rRNA expression and nucleolar activity and organization.

4.5. Conclusion

Tau protein, and more specifically the lowest isoform 0N3R, seems to be involved, through its Ser202/Thr205 residues, in rDNA regulation during cell differentiation. Tau protein may serve a dual function in the nucleolus: one, highlighted by Tau-1 epitope always colocalized with UBTF, and related to the transcription of rRNA genes **(Loomis et al., 1990; Wang et al., 1993; Greenwood and Johnson, 1995; Brady et al., 1995; Thurston et al., 1996**), and the other, involving AT8, only transiently colocalized with UBTF (when the transcription is downregulated or blocked by Act-D), and possibly related to the protection **(Sjöberg et al., 2006; Mansuroglu et al., 2016)** and/or to the organization of the inactive rRNA genes **(Boisvert et al., 2007; Emmott and Hiscox, 2009)**. Moreover, the Ser202/Thr205 residues, with their cell cycle dependent phosphorylation in replicative cells, seems to be involved in mitotic progression. Thus, we identified three different types of Tau detected by Tau-1 and AT8: one with the unphosphorylated Pro189/Gly207 residues (Tau-1) and related to the active rDNA, and the other two with pSer202/Thr205 related to the inactive rDNA, on the one hand, and to the mitotic spindle on the other. Considering the presence/absence of Tau with pSer202/Thr205 in the nucleolus of differentiated/replicative cells, AT8 could be considered a marker of the differentiated status of the neuronal cells.

ACKNOWLEDGEMENTS

Authors thank Denise Greco, and Valeria Coco for the assistance in the experimental procedures with the cell lines, and the University of Catania for the laboratory facilities.

COMPETING INTERESTS

The authors declare no competing or financial interests.

AUTHOR CONTRIBUTIONS

C.F., L.G, and S.S conceived the research, designed the experiments and wrote the manuscript. C.F., L.G., F.B, and S.S. performed immunofluorescence experiments and *MAPT* gene analyses. A.G.D., and V.D. performed and analysed the western blots.

FUNDING

This research did not receive any specific grant from funding agencies in the public, commercial, or not-for-profit sectors.

REFERENCES

Akhmanova A, Verkerk T, Langeveld A, Grosveld F, and Galjart N, 2000. Characterisation of transcriptionally active and inactive chromatin domains in neurons. J Cell Sci 113, 4463-4474.

Anastassova-Kristeva M, 1977. The nucleolar cycle in man. J Cell Sci 25, 103-10.

Andreadis A, 2005. Tau gene alternative splicing: expression patterns, regulation and modulation of function in normal brain and neurodegenerative diseases. Biochim Biophys Acta 1739, 91-103. https://doi.org/ 10.1016/j.bbadis.2004.08.010.

Andres D, Keyser BM, Petrali J, Benton B, Hubbard KS, McNutt PM, and Ray R, 2013. Morphological and functional differentiation in BE(2)-M17 human neuroblastoma cells by treatment with Trans-retinoic acid. BMC Neuroscience 14, 49. https://doi.org/10.1186/1471-2202-14-49.

Avila J, 2009. The Tau code. Front Aging Neurosci. 1, 1. https://doi.org/10.3389/neuro.24.001.2009. eCollection 2009.

Bártová E, Harničarová Horáková A, Uhlířová R, Raška I, Galiová G, Orlova D, and Kozubek S, 2010. Structure and epigenetics of nucleoli in comparison with non-nucleolar compartments. J Histochem Cytochem 58, 391-403. https://doi.org/10.1369/jhc.2009.955435.

Bensaude O, 2011. Inhibiting eukaryotic transcription: Which compound to choose? How to evaluate its activity? Transcription 2, 103-108. https://doi.org/10.4161/trns.2.3.16172.

Bernardi G, 2015. Chromosome architecture and genome organization. Plos One 10, e0143739. https://doi.org/10.1371/journal.pone.0143739.

Biedler JL, Roffler-Tarlov S, Schachner M, and Freedman LS, 1978. Multiple neurotransmitter synthesis by human neuroblastoma cell lines and clones. Cancer Res 38, 3751–3757.

Boisvert FM, van Koningsbruggen S, Navascues J, and Lamond AI, 2007. The multifunctional nucleolus. Nat Rev Mol Cell Biol 8, 574–585. https://doi.org/10.1038/nrm2184.

Braak H, and Braak E, 1991. Neuropathological staining of Alzheimer-related changes. Acta Neuropathol 82, 239-259.

Brady RM, Zinkowski RP, and Binder LI, 1995. Presence of Tau in isolated nuclei from human brain. Neurobiol Aging 16, 479-486.

Buée L, Bussière T, Buée-Scherrer V, Delacourte A, and Hof PR, 2000. Tau protein isoforms, phosphorylation and role in neurodegenerative disorders. Brain Res Rev 33, 95-130.

Bukar Maina M, Al-Hilaly YK, and Serpell LC, 2016. Nuclear Tau and its potential role in Alzheimer's disease. Biomolecules 6, 9. https://doi.org/10.3390/biom6010009.

Carmo-Fonseca M, Mendes-Soares L, and Campos I, 2000. To be or not to be in the nucleolus. Nat Cell Biol. 2, E107-12. https://doi.org/10.1038/35014078.

Conconi A, Widmer RM, Koller T, Sogo JM, 1989. Two different chromatin structures coexist in ribosomal RNA genes throughout the cell cycle. Cell 1989 57, 753-761. https://doi.org/10.1016/0092-8674(89)90790-3.

D'Aquila P, Montesanto A, Mandalà M, Garasto S, Mari V, Corsonello A, Bellizzi D, and Passarino G, 2017. Methylation of the ribosomal RNA gene promoter is associated with aging and age-related decline. Aging Cell 16, 966-975. https://doi.org/10.1111/acel.12603.

D'Alessio A, De Vita G, Calì G, Nitsch L, Fusco A, Vecchio G, Santelli G, Santoro M, and de Franciscis V., 1995. Expression of the RET oncogene induces differentiation of SK-N-BE neuroblastoma cells. Cell growth Differ 6, 1387–1394.

Dauphinais C, 1981. The control of ribosomal RNA transcription in lymphocytes evidence that the rate of chain elongation is the limiting factor. Eur J Biochem 114, 487-492.

Denissov S, Lessard F, Mayer C, Stefanovsky V, van Driel M, Grummt I, Moss T, and Stunnenberg HG, 2011. A model for the topology of active ribosomal RNA genes. EMBO Rep 12, 231-237. https://doi.org/10.1038/embor.2011.8.

Dixit R, Ross JL, Goldman YE, and Holzbaur ELF, 2008. Differential Regulation of Dynein and Kinesin Motor Proteins by Tau. Science 319, 1086–1089. https://doi.org/10.1126/science.1152993.

Emmott E, and Hiscox JA, 2009. Nucleolar targeting: the hub of the matter. EMBO Rep. 10, 231-238. https://doi.org/10.1038/embor.2009.14

Federico C, Cantarella CD, Di Mare P, Tosi S, and Saccone S, 2008. The radial arrangement of the human chromosome 7 in the lymphocyte cell nucleus is associated with chromosomal band gene density. Chromosoma 117, 399-410. https://doi.org/10.1007/s00412-008-0160-x.

Federico C, Dugo K, Bruno F, Longo AM, Grillo A, Saccone S, 2017a. Somatic mosaicism with reversion to normality of a mutated transthyretin allele related to a familial amyloidotic polyneuropathy. Hum Genet 136:867-873. https://doi.org/10.1007/s00439-017-1810-y

Federico C, Pappalardo AM, Ferrito V, Tosi S, and Saccone S, 2017b. Genomic properties of chromosomal bands are linked to evolutionary rearrangements and new centromere formation in primates. Chromosome Res 25, 261-276. https://doi.org/10.1007/s10577-017-9560-1.

Ford E, Voit R, Liszt G, Magin C, Grummt I, and Guarente L, 2006. Mammalian Sir2 homolog SIRT7 is an activator of RNA polymerase I transcription. Genes Dev 20, 1075-1080.

Gil L, Federico C, Pinedo F, Bruno F, Rebolledo AB, Montoya JJ, Olazabal IM, Ferrer I, and Saccone S, 2017. Aging dependent effect of nuclear Tau. Brain Res 1677, 129-137. https://doi.org/10.1016/j.brainres.2017.09.030.

Goedert M, Spillantini MG, Jakes R, Rutherford D, and Crowther RA, 1989. Multiple isoforms of human microtubule-associated protein Tau: sequences and localization in neurofibrillary tangles of Alzheimer's disease. Neuron 3, 519-526.

Goode BL, Denis PE, Panda D, Radeke MJ, Miller HP, Wilson L, and Feinstein SC, 1997. Functional Interactions between the Proline-rich and Repeat Regions of Tau Enhance Microtubule Binding and Assembly. Mol Biol Cell 8, 353-365.

Greenwood JA, and Johnson GV, 1995. Localization and in situ phosphorylation state of nuclear Tau. Exp Cell Res 220, 332-337. https://doi.org/10.1006/excr.1995.1323.

Grummt I, 2007. Different epigenetic layers engage in complex crosstalk to define the epigenetic state of mammalian rRNA genes. Hum Mol Genet 16, R21-27. https://doi.org/10.1093/hmg/ddm020.

Hanger DP, and Noble W, 2011. Functional Implications of Glycogen SynthaseKinase-3-Mediated Tau Phosphorylation. Int J Alz Disease 2011, 352805. https://doi.org/:10.4061/2011/352805

Hayashi Y, Kuroda T, Kishimoto H, Wang C, Iwama A, and Kimura K, 2014. Downregulation of rRNA transcription triggers cell differentiation. PLoS ONE 9(5): e98586. https://doi.org/10.1371/journal.pone.0098586.

Hernàndez-Ortega K, Garcia-Esparcia P, Gil L, Lucas JJ, and Ferrer I, 2015. Altered machinery of protein synthesis in Alzheimer's: from the nucleolus to the ribosome. Brain Pathol 26, 593-605. https://doi.org/10.1111/bpa.12335.

Hua Q, and He RQ, 2003. Tau could protect DNA double helix structure. Biochim Biophys Acta 1645, 205-211.

Ittner LM, Ke YD, Götz J, 2009. Phosphorylated Tau Interacts with c-Jun N-terminal Kinase-interacting Protein 1 (JIP1) in Alzheimer Disease. J Biol Chem 284, 20909-20916. https://doi.org/10.1074/jbc.M109.014472

Jeganathan S, Hascher A, Chinnathambi S, Biernat J, Mandelkow EM, and Mandelkow E, 2008. Proline-directed pseudo-phosphorylation at AT8 and PHF1 epitopes induces a compaction of the paperclip folding of Tau and generates a pathological (MC-1) conformation. J Biol Chem 283, 32066-32076. https://doi.org/10.1074/jbc.M805300200.

Koh CM, Gurel B, Sutcliffe S, Aryee MJ, Schultz D, Iwata T, Uemura M, Zeller KI, Anele U, Zheng Q, et al., 2011. Alterations in nucleolar structure and gene expression programs in prostatic neoplasia are driven by the MYC oncogene. Am J Pathol 178, 1824-34. https://doi.org/10.1016/j.ajpath.2010.12.040.

Leotta CG, Federico C, Brundo MV, Tosi S, and Saccone S, 2014. HLXB9 gene expression, and nuclear location during in vitro neuronal differentiation in the SK-N-BE neuroblastoma cell line. PLoS One 9(8), e105481. https://doi.org/10.1371/journal.pone.0105481.

Loomis PA, Howardt TH, Castleberryt RP, and Binder LI, 1990. Identification of nuclear τ isoforms in human neuroblastoma cells. Proc Natl Acad Sci USA 87, 8422-8426.

Lucchini R, and Sogo JM, 1992. Different Chromatin Structures along the Spacers Flanking Active and Inactive Xenopus rRNA Genes. Mol Cell Biol 12, 4288-4296.

Mangan H, Gailín MÓ, and McStay B, 2017. Integrating the genomic architecture of human nucleolar organizer regions with the biophysical properties of nucleoli. FEBS J. 284, 3977-3985. doi: 10.1111/febs.14108. https://doi.org/10.1111/febs.14108.

Mansuroglu Z, Benhelli-Mokrani H, Marcato V, Sultan A, Violet M, Chauderlier A, Delattre L, Loyens A, Talahari 3, Bégard S, et al., 2016. Loss of Tau protein affects the structure, transcription and repair of neuronal pericentromeric heterochromatin. Scientific Reports 6, 33047. https://doi.org/10.1038/srep33047.

Maugeri G, D'Amico AG, Magro G, Salvatorelli L, Barbagallo GM, Saccone S, Drago F, Cavallaro S, D'Agata V, 2015. Expression profile of parkin isoforms in human gliomas. Int J Oncol 47, 1282-92. doi: 10.3892/ijo.2015.3105

Maugeri G, D'Amico AG, Rasà DM, Reitano R, Saccone S, Federico C, Parenti R, Magro G, and D'Agata V, 2016. Expression profile of wilms tumor 1 (Wt1) isoforms in undifferentiated and all-trans retinoic acid differentiated neuroblastoma cells. Genes Cancer 7, 47-58. https://doi.org/10.18632/genesandcancer.94.

McStay B, 2016. Nucleolar organizer regions: genomic 'dark matter' requiring illumination. Genes Dev 30, 1598–1610. https://doi.org/10.1101/gad.283838.116.

Parlato R, and Kreiner G, 2013. Nucleolar activity in neurodegenerative diseases: a missing piece of the puzzle? J Mol Med (Berl) 91, 541-547. https://doi.org/10.1007/s00109-012-0981-1.

Perry RP, and Kelley DE, 1970. Inhibition of RNA synthesis by actinomycin D: characteristic dose-

response of different RNA specis. J Cell Physiol 76, 127-140. https://doi.org/10.1002/jcp.1040760202.

Qi H, Cantrelle FX, Benhelli-Mokrani H, Smet-Nocca C, Buée L, Lippens G, Bonnefoy E, Galas MC, and Landrieu I, 2015. Nuclear magnetic resonance spectroscopy characterization of interaction of Tau with DNA and its regulation by phosphorylation. Biochemistry 54, 1525-1533. https://doi.org/10.1021/bi5014613.

Qu MH, Li H, Tian R, Nie CL, Liu Y, Han BS, and He RQ, 2004. Neuronal Tau induces DNA conformational changes observed by atomic force microscopy. Neuroreport 15, 2723-2727.

Rossi G, Dalprà L, Crosti F, Lissoni S, Sciacca FL, Catania M, Di Fede G, Mangieri M, Giaccone G, Croci D, and Tagliavini F, 2008. A new function of microtubule-associated protein Tau: involvement in chromosome stability. Cell Cycle 7, 1788-1794. https://doi.org/10.4161/cc.7.12.6012.

Saccone S, Federico C, and Bernardi G, 2002. Localization of the gene-richest and the gene-poorest isochores in the interphase nuclei of mammals and birds. Gene 300, 169-178.

Sanij E, and Hannan RD, 2009. The role of UBF in regulating the structure and dynamics of transcriptionally active rDNA chromatin. Epigenetics 4, 374-82.

Sjöberg MK, Shestakova E, Mansuroglu Z, Maccioni RB, and Bonnefoy E, 2006. Tau protein binds to pericentromeric DNA: a putative role for nuclear Tau in nucleolar organization. J Cell Sci 119, 2025-2034. https://doi.org/10.1242/jcs.02907.

Smirnov E, Cmarko D, Mazel T, Hornáček M, and Raška I, 2016. Nucleolar DNA: the host and the guests. Histochem Cell Biol 145, 359–372. https://doi.org/10.1007/s00418-016-1407-x.

Smith CJ, Anderton BH, Davis DR, and Gallo JM, 1995. Tau isoform expression and phosphorylation state during differentiation of cultured neuronal cells. FEBS Lett 375, 243-248.

Sobol M, Yildirim S, Philimonenko VV, Marášek P, Castaño E, and Hozák P, 2013. UBF complexes with phosphatidylinositol 4,5-bisphosphate in nucleolar organizer regions regardless of ongoing RNA polymerase I activity. Nucleus 4, 478-486. https://doi.org/10.4161/nucl.27154.

Souter S, and Lee G, 2009. Microtubule-associated protein Tau in human prostate cancer cells: isoforms, phosphorylation and interactions. J Cell Bioch 108, 555-564. https://doi.org/10.1002/jcb.22287.

Spicakova T, O'Brien MM, Duran GE, Sweet-Cordero A, and Sikic BI, 2010. Expression and silencing of the microtubule-associated protein Tau in breast cancer cells. Mol Cancer Ther 9, 2970-2981. https://doi.org/10.1158/1535-7163.MCT-10-0780.

Sultan A, Nesslany F, Violet M, Bégard S, Loyens A, Talahari S, Mansuroglu Z, Marzin D, Sergeant N, Humez S, et al., 2011. Nuclear Tau, a key player in neuronal DNA protection. J Biol Chem 286, 4566-4575. https://doi.org/10.1074/jbc.M110.199976.

Takada H, and Kurisaki A, 2015. Emerging roles of nucleolar and ribosomal proteins in cancer, development, and aging. Cell Mol Life Sci 72, 4015-4025. 10.1007/s00018-015-1984-1

Thiry M, and Lafontaine DLJ, 2005. Birth of a nucleolus: the evolution of nucleolar compartments. Trends Cell Biol 15, 194-199. https://doi.org/10.1016/j.tcb.2005.02.007.

Thurston VC, Zinkowski RP, and Binder LI, 1996. Tau as a nucleolar protein in human nonneural cells in vitro and in vivo. Chromosoma 105, 20-30.

Thurston VC, Pena P, Pestell R, and Binder LI, 1997. Nucleolar localization of the Microtubule-Associated Protein Tau in neuroblastomas using sense and anti-sense transfection strategies. Cell Motil Cytoskeleton 38, 100–110.

Torelli UL, Henry PH, Weissman SM, 1968. Characteristics of the RNA synthesized in vitro by the normal human small lymphocyte and the changes induced by phytohemagglutinin stimulation. J Clin Invest 47, 1083-1095.

Violet M, Delattre L, Tardivel M, Sultan A, Chauderlier A, Caillierez R, Talahari S, Nesslany F, Lefebvre B, Bonnefoy E, et al., 2014. A major role for Tau in neuronal DNA and RNA protection in vivo under physiological and hyperthermic conditions. Front Cell Neurosci 8, 84. https://doi.org/10.3389/fncel.2014.00084.

Von Bergen M, Barghorn S, and Biernat J, 2005. Tau aggregation is driven by a transition from random coil to beta sheet structure. Biochim Biophys Acta 1739, 158–166. https://doi.org/10.1016/j.bbadis.2004.09.010.

Wang J-Z, Iqbal IG, and Iqbal k, 2007. Kinases and phosphatases and tau sites involved in Alzheimer neurofibrillary degeneration. Eur J Neurosci 25, 59–68. https://doi.org/10.1111/j.1460-9568.2006.05226.x.

Wang X, Wang D, Zhao J, Qu M, Zhou X, He H, and He R, 2006. The proline-rich domain and the microtubule binding domain of protein Tau acting as RNA binding domains. Protein Pept Lett 13, 679-85.

Wang Y, Loomis PA, Zinkowski RP, and Binder LI, 1993. A novel Tau transcript in cultured human neuroblastoma cells expressing nuclear Tau. J Cell Biol 121, 257–267.

Wang Y, Mandelkow E, 2016. Tau in physiology and pathology. Nat Rev Neurosci 17, 5-21. https://doi.org/10.1038/nrn.2015.1.

Wei Y, Qu MH, Wang XS, Chen L, Wang DL, Liu Y, Hua Q, and He RQ, 2008. Binding to the minor groove of the double-strand, Tau protein prevents DNA from damage by peroxidation. PLoS One 3, e2600. https://doi.org/10.1371/journal.pone.0002600.

Weingarten MD, Lockwood AH, Hwo SY, and Kirschner MW, 1975. A protein factor essential for microtubule assembly. Proc Natl Acad Sci USA 72, 1858-1862.

FIGURE LEGENDS

Fig. 1. Differentiation of the SK-N-BE cells following exposure for 12 days to retinoic acid (RA). (A, B) Change in cell morphology induced by RA, and visible as very long cytoplasmic extensions among differentiated cells. (C, D) Expression of the protein GAP-43, not present in the replicative cells. (E, F) NOR formation: nucleolus of replicative cells shows many active NORs (Nucleolar Organizing Regions). In differentiated cells NORs decrease in number and become larger. (G, H) The nucleolar specific fibrillarin protein is largely present in the nucleolus of replicative cells, but absent in the differentiated ones. In (C), (D), (G), and (H), nuclei were stained with DAPI (blue). Scale bars: 20, 50 and 10 µm in A, B, and C/D respectively. 5 µm in E-F-G-H.

Fig. 2. Expression level of the rRNA gene cluster. (A) Schematic representation of the rDNA start region, with the position (vertical arrows) of the amplified segments used to evaluate the rDNA transcriptional level: non-transcribed promoter (nt-Pr), transcribed ETS (t-ETS) and transcribed 18S gene (t-18S). Drawing is not to scale. (B) qRT-PCR amplification plot obtained with the three regions (nt-Pr, t-ETS, and t-18S) in the replicative and differentiated SK-N-BE cells. ACTB was used as endogenous controls. (C) *Upper*: graph with the ratio of the rRNA transcriptional level in the differentiated cells with respect to the replicative SK-N-BE cells. t-ETS value indicates the drastically reduced transcriptional level of the rDNA in differentiated cells (*** $p < 0.001$). RQ diff: RQ in differentiated cells; RQ repl: RQ in replicative cells; each bar graph shows the ± standard error of the mean (SEM). *Bottom*: size of the amplified segments verified after qRT-PCR with a 2% agarose gel electrophoresis. R, and D: replicative and differentiated cells, respectively; bp: base pairs.

Fig. 3. Tau protein in the SK-N-BE cells. Localization, by IF, of the Tau epitopes Tau-1 and AT8 in replicative and differentiated cells. Representative nuclei (stained in blue with DAPI) are shown. (A) and (B) show the localization of Tau-1 and AT8, respectively, in the replicative cells. (C) and (D) show the distribution of Tau-1 and AT8, respectively, in the differentiated cells. (A’ to D’) and (A’’ to D’’) show the same nuclei in (A to D) with the DAPI staining (blue) and the IF signals (green), respectively. Scale bars: 5 µm.

Fig. 4. Transcriptional block induced by Act-D, and Tau protein distribution. Detection of Tau protein (epitopes Tau-1 and AT8, green signals) after 1 hour of Act-D exposure of the cells (C, D) compared to replicative (A, B) and differentiated (E, F) cells. In (B), two metaphases (m) with a large amount of AT8 (green signals) are visible. In (D), a metaphase (m) with a low amount of AT8 (green signals) is visible. (a to f) Nuclei with greater magnification and (a' to f') schematic representation of the

nucleolar distribution of Tau epitopes in the cell conditions shown in (A) to (F), respectively. Letter indications (a to f and a' to f') follow the upper panels (A) to (F), respectively. (G to L) Tau-1 and AT8 epitopes during mitosis. (G) and (I) Tau-1 in the replicative cells. (H) and (J) AT8 in the differentiated cells. (K) and (L) Tau-1 and AT8, in the replicative SK-N-BE cells after 1 hour of Act-D exposure. (P) and (T) localization of Tau-1 and AT8 (green signals), respectively, with respect to UBTF (red signals). Tau-1 and AT8 were detected by FITC conjugated secondary antibody (green signals). Nuclei and chromosomes were stained with DAPI (blue). The red arrow (panel J) indicates the nucleolus (nu) without AT8. nu: nucleolus; m: metaphase; an: anaphase. Scale bars: 5 µm.

Fig. 5. Tau protein in the lymphocytes. Tau-1 and AT8 epitopes were localized in human lymphocytes before (A, B), and after (D, E) 72 hours PHA exposure. Fibrillarin protein IF detection was included as a control of the PHA induced (F) *vs* uninduced cells (C), as well the transcriptional level of the gene (G). The different epitopes of Tau and FBL were detected by FITC conjugated secondary antibody (green signals) and nuclei were stained with DAPI (blue). At the bottom of each panel, a dual colour IF with detection of UBTF (red signals) and Tau-1/AT8/FBL (green signals) was shown. (G) FBL transcriptional level in the lymphocytes cultured with or without PHA obtained by qRT-PCR and ACTB as endogenous control. The relative quantifications (RQ) are represented as mean ± SEM. *** $p < 0.001$. PHA: phytohaemagglutinin; FBL: fibrillarin; UBTF: upstream binding transcription factor. Scale bars: 5 µm.

Fig. 6. Alternative splicing of the *MAPT* gene in the SK-N-BE cells. **(A)** Exon organization of *MAPT* gene. Blue exons are constitutive and the red ones are alternatively spliced in neuronal cells. Grey exons are generally not present in the transcript of neuronal cells. The size of each exon is indicated at the top of the scheme and corresponds to the coding sequence. The indicated size of the exon 1 (133*) begins with the start codon and that of exon 13 (213*) finishes with the stop codon. Primers used for RT-PCR (see Table 1 for the sequences) are indicated at the bottom: blue and red arrows indicate the position of the forward (F) and reverse (R) primers, respectively. (B) and (C) Electrophoretic results obtained by RT-PCR with the primers indicated in the upper part. M, indicates the marker DNA. R and D indicate replicative and differentiated cells, respectively. At the bottom, the expected sizes of the amplified segments are indicated. The obtained fragments or faintly visible are indicated in bold. The fragments not observed are indicated in brackets. On the bottom right of panel (C), the Tau isoforms are indicated in correspondence to the size of the amplified DNA obtainable with F1-R11 and F1-R13 primers. The underlined isoform 1N3R, with a size similar to the 0N4R, is not present in the cells, as demonstrated with qRT-PCR (see **Fig. 7**).

Fig. 7. Transcriptional pattern of the *MAPT* gene. (A) and (B) qRT-PCR involving the spliced exons 2-3 (0N, 1N, 2N repeats) and exon 10 (3R, 4R repeats), respectively, in replicative and differentiated SK-N-BE cells. 0N, 1N, 2N, 3R and 4R amplification plots were obtained with primers F1/4-R5, F2/4-R4, F2/3-R4, F9/11-R12 and F9/10-R12, respectively (primer sequences in **Table 1**). (C) Histogram generated with values of $2^{-\Delta\Delta Ct}$. The relative quantifications (RQ) are represented as mean ± SEM.

Fig. 8. Expression level of the Tau protein. Representative immunoblots with signals detected by Tau-5 (A), Tau-1 (B) and AT8 (C) antibodies on cell homogenates from replicative SK-N-BE cells (Repl.), differentiated SK-N-BE cells (Diff.) and replicative SK-N-BE cells after 1 hour of Act-D treatment (Repl.+Act-D). The bar graphs show the results of three independent experiments. Relative band density was quantified using ImageJ software and the protein levels were expressed as arbitrary units obtained after normalization to β-tubulin (D), which was used as a loading control. Data are expressed as mean ± SEM. ***$p < 0.001$, and **$p < 0.01$ *vs* replicative cells as determined by one-way ANOVA followed by Tukey post hoc test.

Table 1. PCR primers used to amplify the reverse transcribed mRNA of the *MAPT* gene and primers for qRT-PCR to amplify rRNA transcripts.

Primer	***Type***	***Gene***	***Location***	***Nucleotide sequence (5'-3')***
F1	Forward	*MAPT*	*Exon-1*	AACCAGGATGGCTGAGCCCC
F2	Forward	*MAPT*	*Exon-2*	CGGATCTGAGGAACCGGGCTC
F4	Forward	*MAPT*	*Exon-4*	TGAAGAAGCAGGCATTGGAG
R4	Reverse	*MAPT*	*Exon-4*	GTGACCAGCAGCTTCGTCTT
R5	Reverse	*MAPT*	*Exon-5*	ATCGCTTCCAGTCCCGTCT
R7	Reverse	*MAPT*	*Exon-7*	ATCCTGGTGGCGTTGGCCTG
R9	Reverse	*MAPT*	*Exon-9*	CTTCCCGCCTCCCGGCTGGTG
F9/10	Forward	*MAPT*	*Exon-9/10*	CGGGAAGGTGCAGATAATTAA
F9/11	Forward	*MAPT*	*Exon-9/11*	AGGCGGGAAGGTGCAAATA
R11	Reverse	*MAPT*	*Exon-11*	TGCTCAGGTCAACTGGTTTG
R12	Reverse	*MAPT*	*exon-12*	CCCAATCTTCGACTGGACTC
R13	Reverse	*MAPT*	*exon-13*	CAAACCCTGCTTGGCCAGGGA
F1/4	Forward	*MAPT*	Exon-1/4	GCTGGCCTGAAAGCTGAAG
F2/4	Forward	*MAPT*	Exon-2/4	CAACAGCGGAAGCTGAAGAA
F2/3	Forward	*MAPT*	Exon-2/3	ACTCCAACAGCGGAAGATGT
ntPr-F	Forward	*rRNAs*	Promoter (42805[(a)])	GTGTGTCCTTGGGTTGACCA[(b)]
ntPr-R	Reverse	*rRNAs*	Promoter (42975[(a)])	CCGACTCGGAGCGAAAGATA[(b)]
tETS-F	Forward	*rRNAs*	ETS (9[(a)])	GCTGTCCTCTGGCGAC
tETS -R	Reverse	*rRNAs*	ETS (120[(a)])	CGGCAGGCGGCTCAAG
t18S-F	Forward	*rRNAs*	*18S rRNA* (5340[(a)])	CCCTGCCCTTTGTACACACC
t18S-R	Reverse	*rRNAs*	*18S rRNA* (5520[(a)])	CCTTCCGCAGGTTCACCTAC
FBL-F	Forward	*FBL*	*exon-5*[(c)]	TGGACCAGATCCACATCAAA[(d)]
FBL-R	Reverse	*FBL*	*exon5/6*[(c)]	GACTAGACCATCCGGACCAA[(d)]
FH1-ACTB	Forward	*ACTB*	*Exon-2*	GACGACATGGAGAAAATCTG[(e)]
RH1-ACTB	Reverse	*ACTB*	*Exon-2/3*	ATGATCTGGGTCATCTTCTC[(f)]

MAPT primers are from **Souter and Lee 2009** and **Spicakova et al. 2010**. ETS: External transcribed spacer. (a) primer position (the first nucleotide) in the "Human ribosomal DNA complete repeating unit" sequence

(GenBank: U13369.1). (b) from **Ford et al. 2006**. (c) GenBank: NM001436.3. (d) from **Koh et al. 2011**. (e) and (f) from Sigma-Aldrich (cat. n. HA04662150 and HA04662151, respectively).

Highlights:

Phosphorylation of the Ser202/Thr205 residues (AT8 epitope) occurs in the nucleolus of transcriptionally inhibited cells.

Only the smallest isoform, 0N3R, of the Tau protein is present in the SK-N-BE neuroblastoma cell line.

The expression of the nuclear Tau increases during neuronal cell differentiation.

Tau protein (Tau-1 epitope) colocalizes with the upstream binding transcription factor in the nucleolus.

PHA-induced lymphocytes and neuroblastoma replicative cells show a similar nuclear Tau distribution.

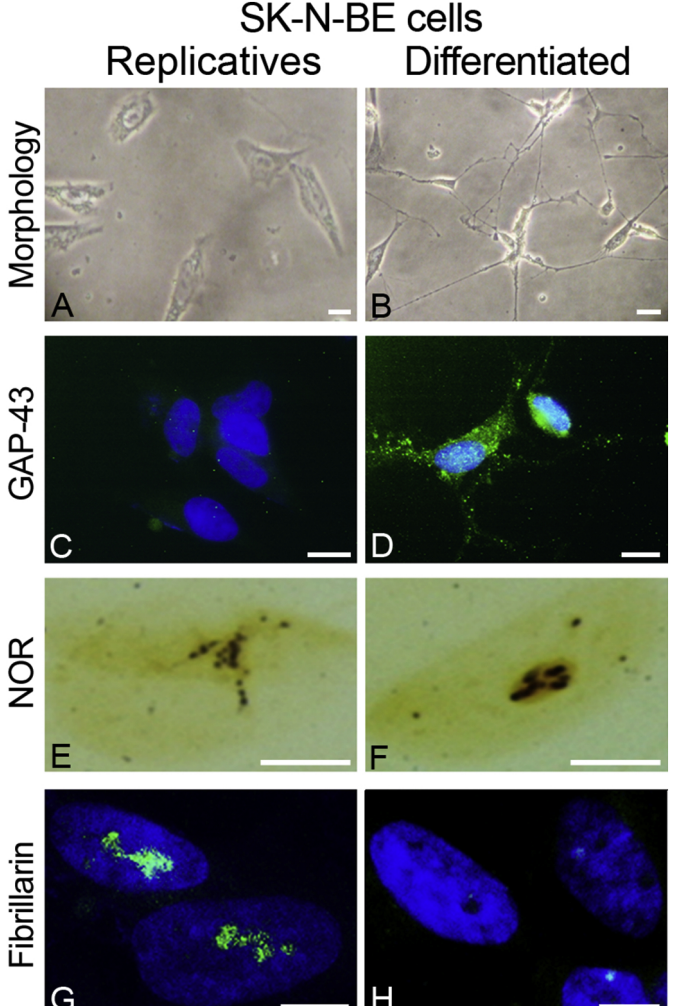
SK-N-BE cells
Replicatives
Differentiated
Morphology
GAP-43
NOR
Fibrillarin
A
B
C
D
E
F
G
H

Figure 1

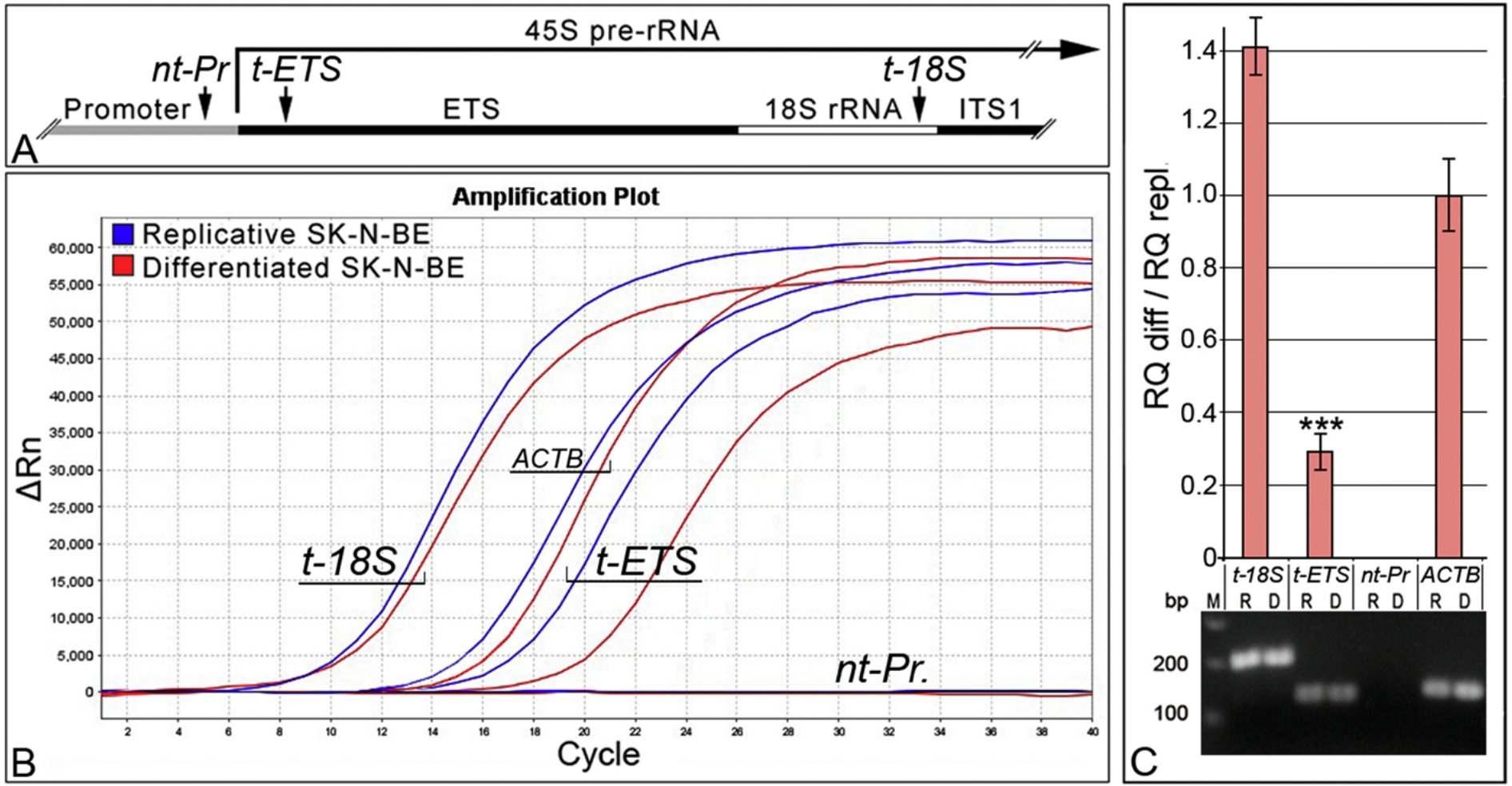
45S pre-rRNA
nt-Pr
t-ETS
t-18S
Promoter
ETS
18S rRNA
ITS1
A
Amplification Plot
Replicative SK-N-BE
Differentiated SK-N-BE
ΔRn
ACTB
t-18S
t-ETS
nt-Pr.
Cycle
B
RQ diff / RQ repl.
***
t-18S
t-ETS
nt-Pr
ACTB
bp
M
R
D
200
100
C

Figure 2

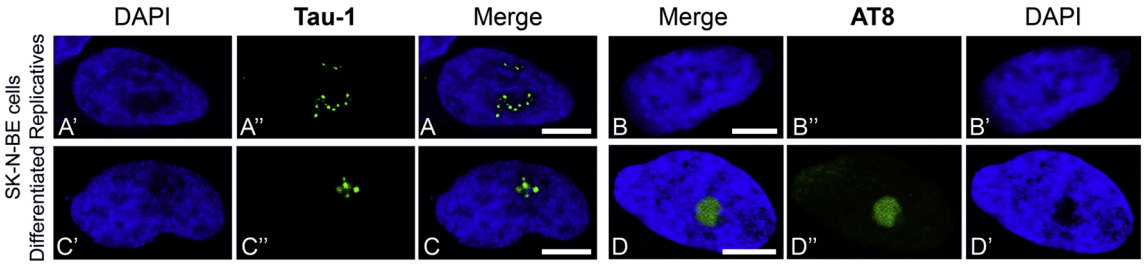
DAPI
Tau-1
Merge
Merge
AT8
DAPI
SK-N-BE cells
Differentiated Replicatives
A'
A''
A
B
B''
B'
C'
C''
C
D
D''
D'

Figure 3

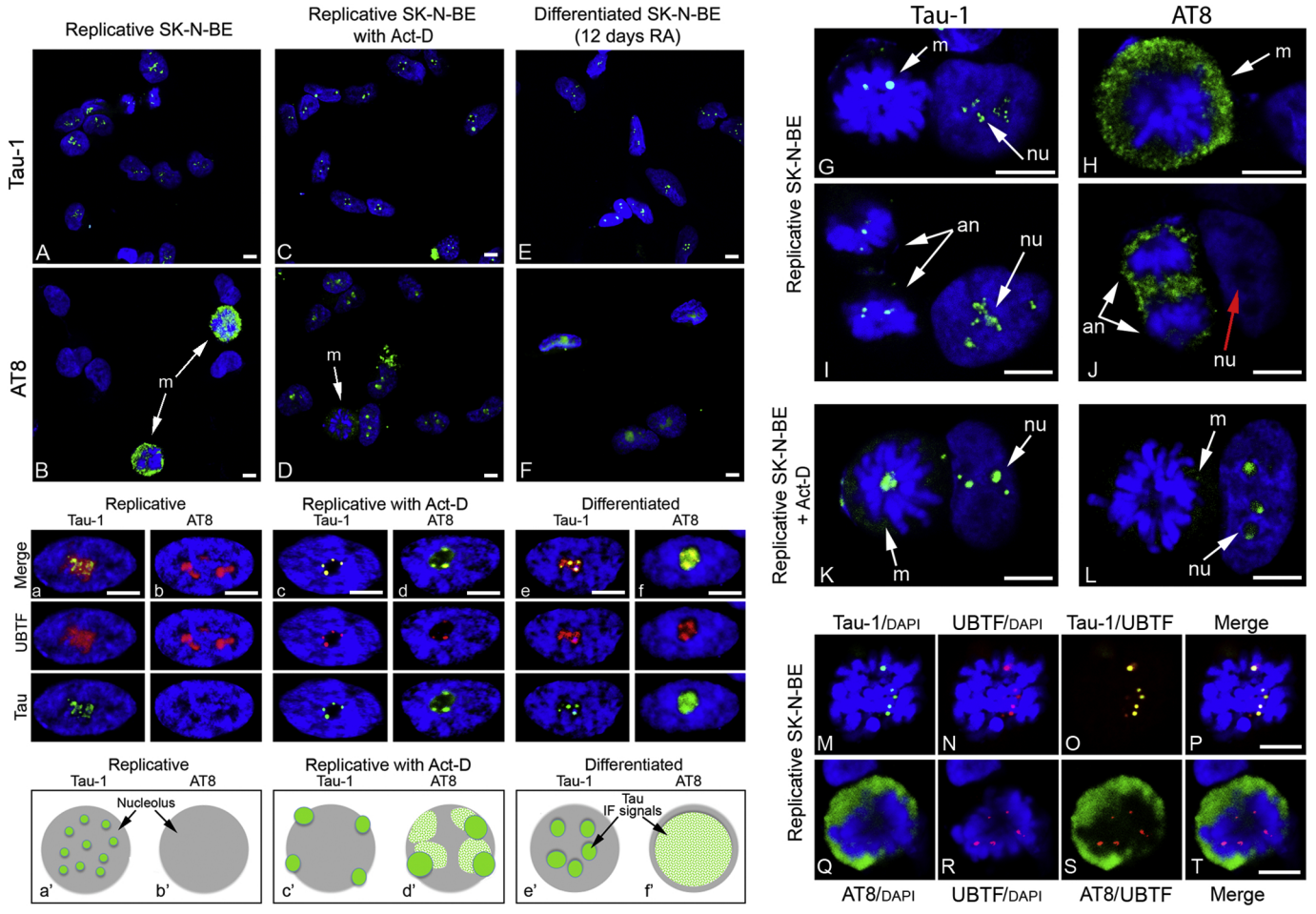
Replicative SK-N-BE
Replicative SK-N-BE with Act-D
Differentiated SK-N-BE (12 days RA)
Tau-1
AT8
A
B
C
D
E
F
m
Replicative
Replicative with Act-D
Differentiated
Merge
UBTF
Tau
a
b
c
d
e
f
Nucleolus
Tau IF signals
a'
b'
c'
d'
e'
f'
Tau-1
AT8
Replicative SK-N-BE
Replicative SK-N-BE + Act-D
G
H
I
J
K
L
nu
an
Tau-1/DAPI
UBTF/DAPI
Tau-1/UBTF
Merge
AT8/DAPI
AT8/UBTF
M
N
O
P
Q
R
S
T

Figure 4

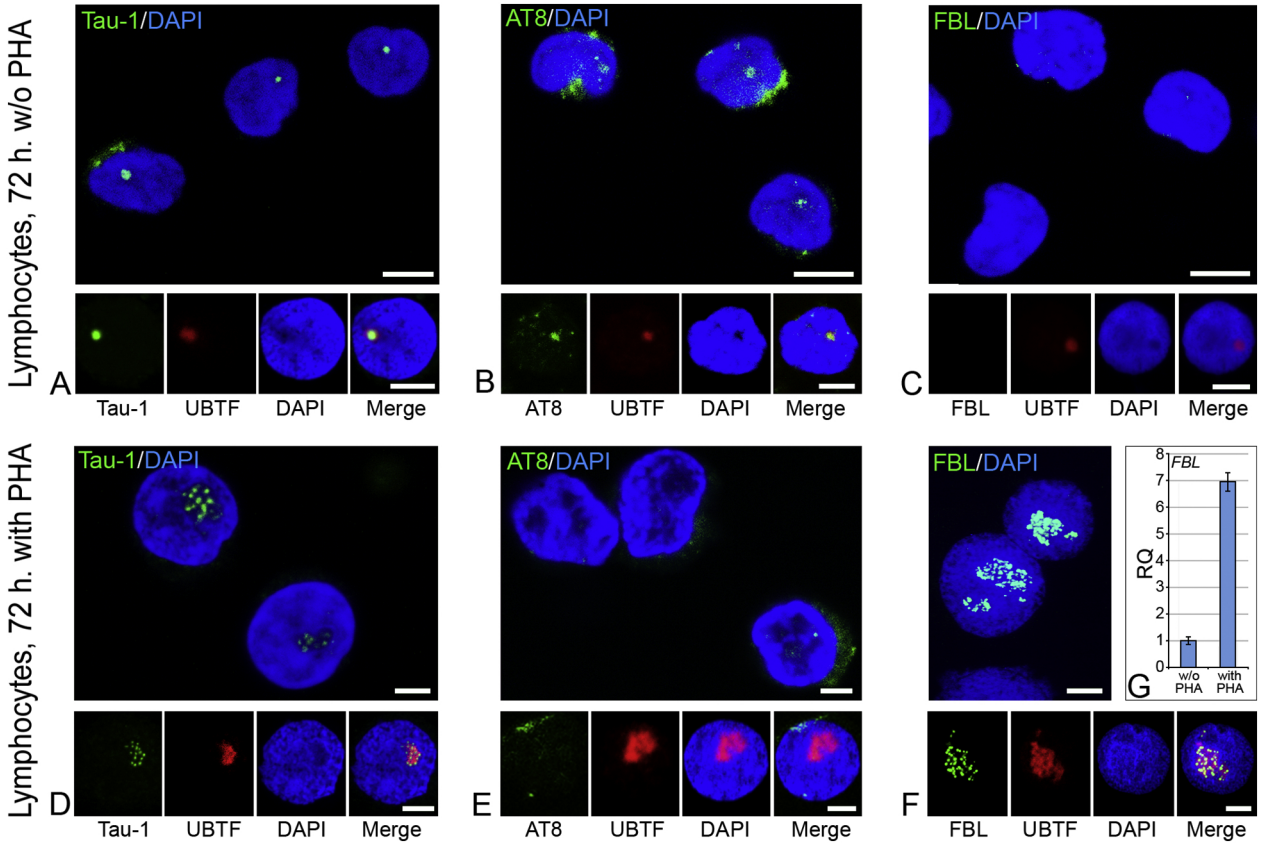
Lymphocytes, 72 h. w/o PHA
Tau-1/DAPI
AT8/DAPI
FBL/DAPI
A
Tau-1
UBTF
DAPI
Merge
B
AT8
UBTF
DAPI
Merge
C
FBL
UBTF
DAPI
Merge
Lymphocytes, 72 h. with PHA
Tau-1/DAPI
AT8/DAPI
FBL/DAPI
D
Tau-1
UBTF
DAPI
Merge
E
AT8
UBTF
DAPI
Merge
F
FBL
UBTF
DAPI
Merge
G
FBL
RQ
0
1
2
3
4
5
6
7
8
w/o PHA
with PHA

Figure 5

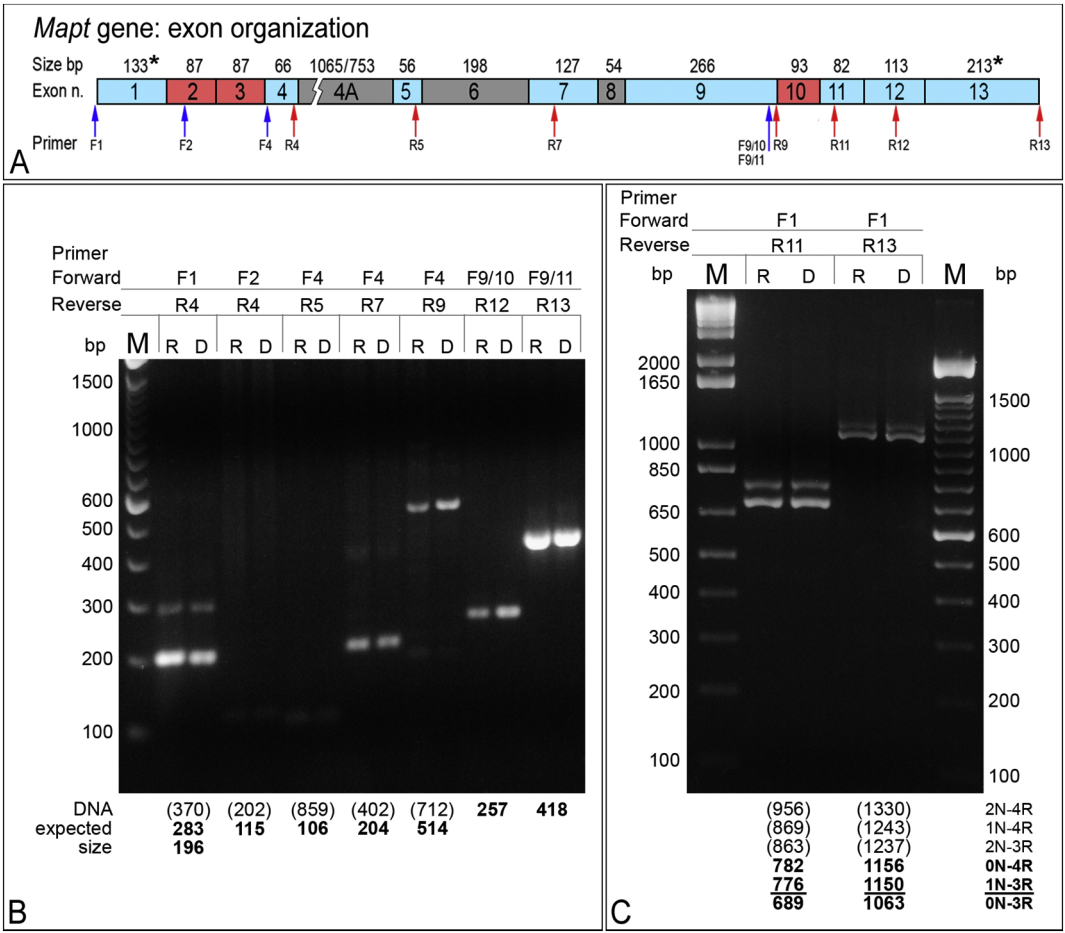
Mapt gene: exon organization
Size bp
133*
87
87
66
1065/753
56
198
127
54
266
93
82
113
213*
Exon n.
1
2
3
4
4A
5
6
7
8
9
10
11
12
13
Primer
F1
F2
F4
R4
R5
R7
F9/10
F9/11
R9
R11
R12
R13
A
Primer
Forward
F1
F2
F4
F4
F4
F9/10
F9/11
Reverse
R4
R4
R5
R7
R9
R12
R13
bp
M
R
D
1500
1000
600
500
400
300
200
100
DNA
expected
size
(370)
283
196
(202)
115
(859)
106
(402)
204
(712)
514
257
418
B
Primer
Forward
F1
F1
Reverse
R11
R13
bp
M
R
D
2000
1650
1000
850
650
500
400
300
200
100
(956)
(869)
(863)
782
776
689
(1330)
(1243)
(1237)
1156
1150
1063
2N-4R
1N-4R
2N-3R
0N-4R
1N-3R
0N-3R
C

Figure 6

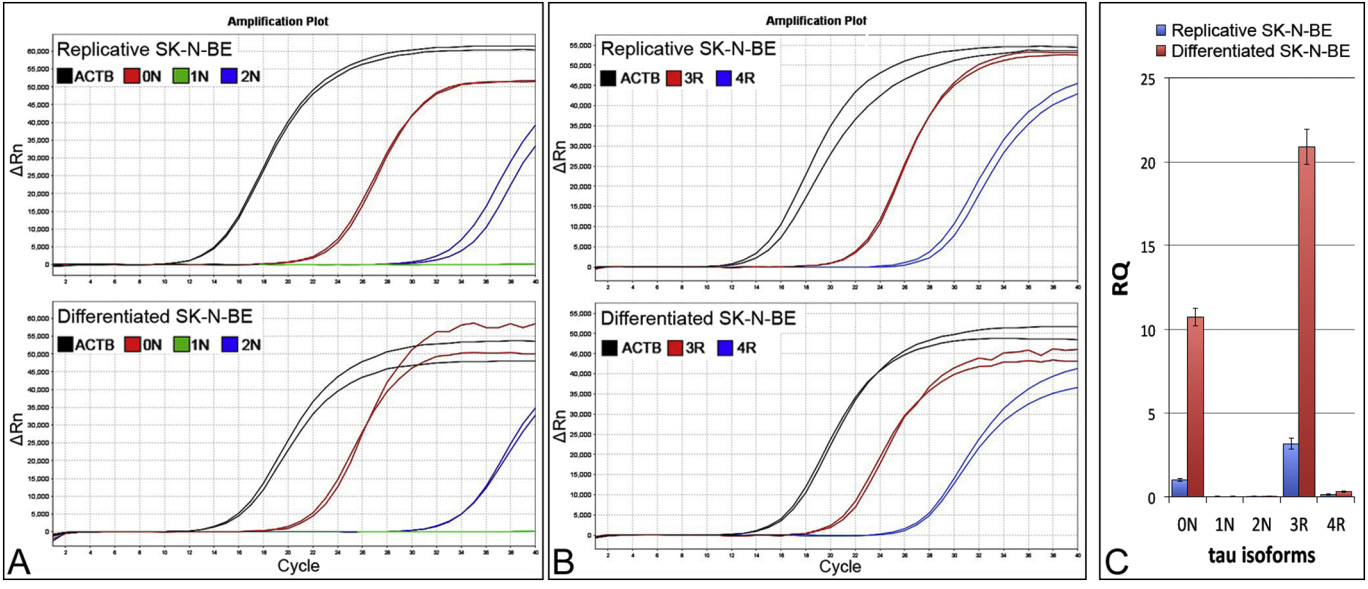
Amplification Plot
Replicative SK-N-BE
ACTB 0N 1N 2N
ΔRn
Differentiated SK-N-BE
ACTB 0N 1N 2N
ΔRn
A
Cycle
Amplification Plot
Replicative SK-N-BE
ACTB 3R 4R
ΔRn
Differentiated SK-N-BE
ACTB 3R 4R
ΔRn
B
Cycle
Replicative SK-N-BE
Differentiated SK-N-BE
RQ
0N 1N 2N 3R 4R
tau isoforms
C

Figure 7

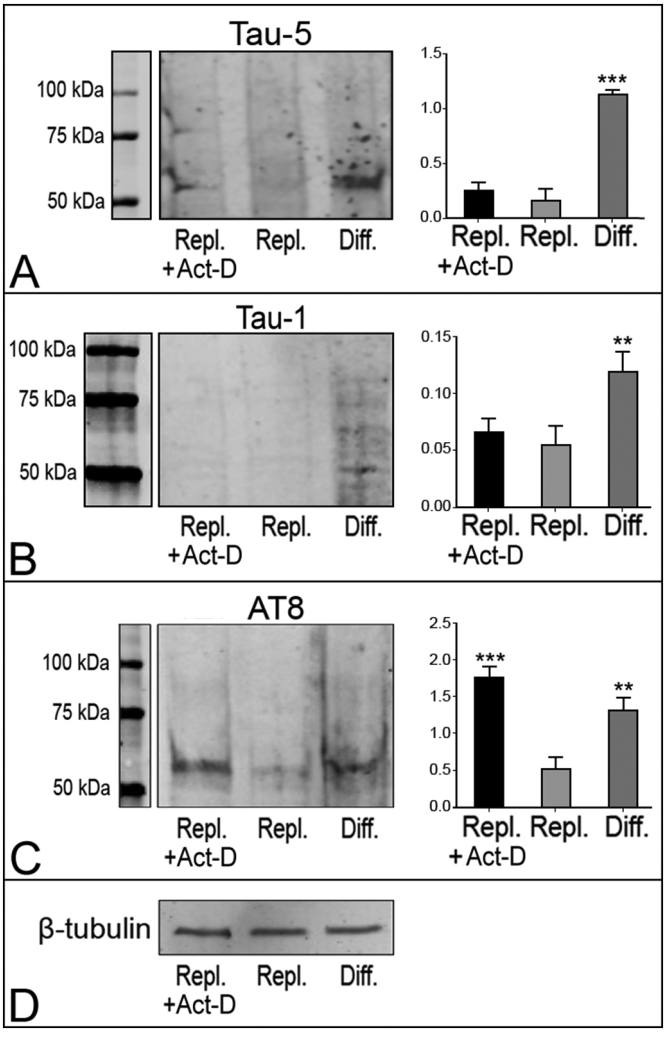

Figure 8